PERFORMANCE ANALYSIS OF KNOCK DETECTORS

M. Zadnik*, **F. Vincent**†, **F. Galtier**‡, **R.A. Vingerhoeds**‡

* *AMPERE, 42 av. du Général de Croutte, 31100 Toulouse, France, martin.zadnik@siemens.com*
† *ENSICA, 1 pl. Émile Blouin, 31056 Toulouse, France, vincent@ensica.fr*
‡ *Siemens VDO Automotive, 1 av. Paul Ourliac, 31036 Toulouse, France, {frederic.galtier, robertus.vingerhoeds}@siemens.com*

Keywords: engine knock, knock signal model, detection, receiver operating characteristic

Abstract

This paper examines performance of the knock detection technique typically used in engine control systems, and the margin for possible improvement. We introduce a knock signal model and obtain an analytical result for the associated receiver operating characteristic of the standard knock detector. To show the improvement potential, we derive the theoretical upper bound of performance. A special case with unknown model parameters is also considered. Numerical results stimulate the research of improved detectors.

1 Introduction

A high compression ratio and a proper spark timing advance are necessary to attain good efficiency of internal combustion gasoline engines. Both parameters are limited by the apparition of knock which is a spontaneous ignition of unburned air-fuel mixture that occurs after ignition by spark plug [1]. Knock consequences are harmful, from excessive emission of pollutants, efficiency decrease, to engine damage [2]. Its detection and prevention are thus an important part of engine control.

For economic reasons, the direct method of measuring knock by in-cylinder pressure transducers is usually replaced by exploiting the vibration signal from one or more accelerometers mounted on engine block surface. Knock being constituted of several resonances determined by cylinder geometry [3], the standard treatment is to apply a band-pass filter followed by computation of signal energy in a predefined time window. The result is compared to base engine noise to make a decision whether knock is present or not. Parameters of the treatment like the resonance to choose, filter frequency and time window are determined for each engine type during calibration phase.

In this paper, we investigate the detection performance resulting from the described knock signal processing scheme by means of detection theory. Contrary to [4] where a similar analysis is performed by simulation on real training data, analytical results give access to arbitrary false alarm rates as we are not limited by sample data size. The analysis is based on a simple signal model including some unknown parameters. The detection performance is compared to that of the optimal Neyman-Pearson test which gives the theoretical upper limit for performance of any real world detector. The gap between the two curves shows how much place there is left for possible improvement of actual knock detection method.

The paper is organised as follows. In Section 2, we introduce the signal model. Section 3 gives the associated optimal Neyman-Pearson detector performance. The case where some model parameters are unknown is discussed in Section 4. We derive the performance of the standard knock detection system in Section 5. A numerical example is given in Section 6, before the paper is concluded in Section 7.

2 Knock signal model

Time-frequency analysis of knock vibrations clearly shows a multi-frequency signal structure [5]. It also reveals that resonance frequencies decrease with time which is due to temperature and sound speed decrease. Theoretical analysis and experiments show that a linear frequency modulation (i.e. a 2nd order polynomial phase) is a good approximation [6]. In a similar manner as in [7], we write the signal model as a sum of P resonances in zero mean white Gaussian additive noise of variance σ^2:

$$x(t) = s(t) + n(t) =$$
$$= \sum_{p=1}^{P} a_p\, w_p(t) \cos\left(2\pi(\alpha_p t^2 + \beta_p t) + \phi_p\right) + n(t). \quad (2.1)$$

The normalised envelope functions w_p have two parameters describing time scaling and instant of knock begin:

$$w_p(t) = \frac{t - t_{0,p}}{\tau_p} \exp\left(-\frac{t - t_{0,p}}{\tau_p} + 1\right) \Theta\left(t - t_{0,p}\right), \quad (2.2)$$

$\Theta(t)$ being the Heaviside unit step function. The form of envelope functions is shown in figure 1. Each resonance thus has a six-element parameter vector $\boldsymbol{\theta}_p = [a_p, \alpha_p, \beta_p, \phi_p, t_{0,p}, \tau_p]^T$. The sampled signal written as a vector is $\mathbf{x} = [x(0), \ldots, x(N-1)]^T = \mathbf{s} + \mathbf{n}$.

3 Neyman-Pearson performance limit

We formulate the knock detection as a two hypothesis testing problem:

$$\begin{aligned} \mathcal{H}_0 &: \mathbf{x} = \mathbf{n} && \text{(no knock)}, \\ \mathcal{H}_1 &: \mathbf{x} = \mathbf{s} + \mathbf{n} && \text{(knock is present)}. \end{aligned} \quad (3.1)$$

If all the model parameters are known, the optimal test in the sense of maximising the probability of detection P_d for a given

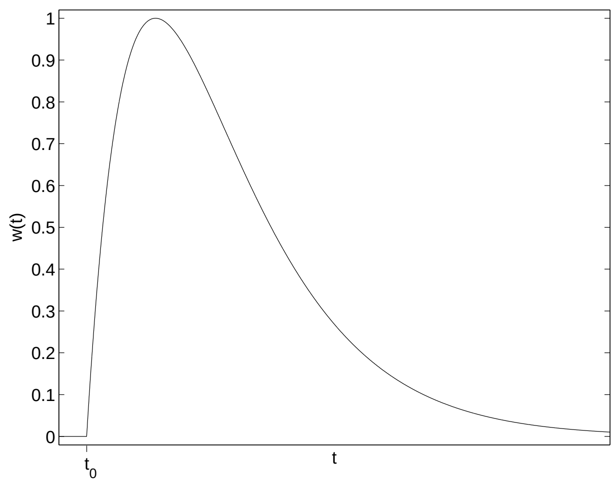

Figure 1: Envelope function given by equation (2.2).

probability of false alarm P_{fa} is the Neyman-Pearson (NP) likelihood ratio test [8]:

$$\text{decide } \mathcal{H}_1 \text{ if} \quad L_{np}(\mathbf{x}) = \frac{p(\mathbf{x};\mathcal{H}_1)}{p(\mathbf{x};\mathcal{H}_0)} > \gamma \tag{3.2}$$

where $p(\mathbf{x};\mathcal{H}_i)$ is the probability density function (PDF) of data $\mathbf{x}$ under i-th hypothesis. For a given signal-to-noise ratio, the threshold γ parametrises the receiver operating characteristic (ROC) curve as $P_{fa}(\gamma) = \Pr[L_{np}(\mathbf{x}) > \gamma;\mathcal{H}_0]$, $P_d(\gamma) = \Pr[L_{np}(\mathbf{x}) > \gamma;\mathcal{H}_1]$. These two probabilities can be analytically calculated. The PDFs to be inserted in (3.2) are

$$p(\mathbf{x};\mathcal{H}_0) = \frac{1}{(2\pi\sigma^2)^{\frac{N}{2}}} \exp\left(-\frac{\mathbf{x}^T\mathbf{x}}{2\sigma^2}\right), \tag{3.3}$$

$$p(\mathbf{x};\mathcal{H}_1) = \frac{1}{(2\pi\sigma^2)^{\frac{N}{2}}} \exp\left(-\frac{(\mathbf{x}-\mathbf{s})^T(\mathbf{x}-\mathbf{s})}{2\sigma^2}\right). \tag{3.4}$$

Since taking a monotonous function of $L_{np}(\mathbf{x})$ does not change the test, we can use the equivalent test statistic

$$\text{decide } \mathcal{H}_1 \text{ if} \quad T_{np}(\mathbf{x}) = \sigma^2 \ln L_{np}(\mathbf{x}) + \frac{1}{2}\mathbf{s}^T\mathbf{s} = = \mathbf{x}^T\mathbf{s} > \gamma' \tag{3.5}$$

which is found to be $T_{np}(\mathbf{x}) \sim \mathcal{N}(0,\sigma^2 E)$ under $\mathcal{H}_0$ and $T_{np}(\mathbf{x}) \sim \mathcal{N}(E,\sigma^2 E)$ under $\mathcal{H}_1$, where we defined the signal energy $E = \mathbf{s}^T\mathbf{s}$, and $\mathcal{N}(\mu,\sigma^2)$ denotes a normal distribution with mean μ and variance σ^2. Note that the form of the test as written in (3.5) corresponds to computing the correlation of measured data with signal model. Like the standard treatment discussed in section 5, it is an energy detector but here only the contribution of the useful signal part is extracted. Finally, we find

$$P_d(\gamma') = Q\left(\frac{\gamma' - E}{\sqrt{\sigma^2 E}}\right), \quad P_{fa}(\gamma') = Q\left(\frac{\gamma'}{\sqrt{\sigma^2 E}}\right) \tag{3.6}$$

where $Q(x) = \int_x^\infty \frac{1}{\sqrt{2\pi}} \exp(-\frac{t^2}{2})\mathrm{d}t$ is the right-tail probability function.

In practice, signal parameters are not all known and the Neyman-Pearson test cannot directly be applied. Replacing the true parameter values by their estimates degrades detection performance and the NP detector can be seen as the upper limit of performance that any detector can reach.

4 Case of unknown amplitudes and phases

We now consider the situation where the signal parameters are all known except the resonance amplitudes a_p and phases ϕ_p. This is equivalent to assuming that the knock signal has a fixed form but the intensity of each resonance can vary. Although without any proof of optimality similar to that of the NP test, the standard approach is to replace the unknown parameters by their maximum likelihood (ML) estimates, which is known as the generalised likelihood ratio test (GLRT).

We rewrite $s(t)$ from (2.1) as

$$s(t) = \sum_{p=1}^{P} \left[A_p\, w_p(t) \cos\left(2\pi(\alpha_p t^2 + \beta_p t)\right) + \right.$$
$$\left. + B_p\, w_p(t) \sin\left(2\pi(\alpha_p t^2 + \beta_p t)\right)\right] \tag{4.1}$$

with $A_p = a_p \cos(\phi_p)$, $B_p = -a_p \sin(\phi_p)$. Introducing the unknown parameter vector $\mathbf{a} = [A_1, B_1, \ldots, A_P, B_P]^T$, we can write

$$\mathbf{x} = \mathbf{S}\mathbf{a} + \mathbf{n} \tag{4.2}$$

where the structure of the $N \times 2P$ matrix $\mathbf{S}$ is obvious from equation (4.1). The ML estimate of $\mathbf{a}$ is $\hat{\mathbf{a}} = (\mathbf{S}^T\mathbf{S})^{-1}\mathbf{S}^T\mathbf{x}$. The detection can be reformulated as testing whether $\mathbf{a} = \mathbf{0}$ ($\mathcal{H}_0$) or $\mathbf{a} \neq \mathbf{0}$ ($\mathcal{H}_1$).

Replacing $\mathbf{s}$ by $\mathbf{S}\hat{\mathbf{a}}$ and proceeding as in section 3, we obtain

$$\text{decide } \mathcal{H}_1 \text{ if} \quad T_{glrt}(\mathbf{x}) = \mathbf{x}^T\mathbf{S}(\mathbf{S}^T\mathbf{S})^{-1}\mathbf{S}^T\mathbf{x} > \gamma'. \tag{4.3}$$

The test is thus a projection of measured data onto the signal subspace. In this case, the test statistic is found to be chi-squared distributed with $2P$ degrees of freedom [8]. The distribution is central under $\mathcal{H}_0$ and noncentral under $\mathcal{H}_1$, the noncentrality parameter being $\lambda = \frac{E}{\sigma^2}$. Hence, the ROC curve can be calculated from

$$P_d(\gamma') = Q_{\chi'^2_{2P}(\lambda)}(\gamma'), \quad P_{fa}(\gamma') = Q_{\chi^2_{2P}}(\gamma') \tag{4.4}$$

where the two Q-functions denote the corresponding right-tail probabilities.

5 Bandpass filter energy detector

As stated before, the classical knock detector compares the bandpass filter output energy to a threshold. We suppose that the filter can be written in a finite impulse response form. The filtered knock signal is

$$\begin{aligned} \mathbf{x}_f &= \mathbf{H}\mathbf{x} = \mathbf{n}_f && \text{under } \mathcal{H}_0 \\ \mathbf{x}_f &= \mathbf{H}\mathbf{x} = \mathbf{s}_f + \mathbf{n}_f && \text{under } \mathcal{H}_1 \end{aligned} \tag{5.1}$$

where $\mathbf{H}$ is the filtering matrix. Let the filtered noise covariance matrix and its diagonalisation be $\mathbf{C} = \mathrm{E}[\mathbf{n}_f\mathbf{n}_f^T] = \mathbf{U}^T\mathbf{\Lambda}\mathbf{U}$. For convenience, we now define $\mathbf{x}_u = \mathbf{U}\mathbf{x}_f = \mathbf{s}_u + \mathbf{n}_u$ and therefore $\mathbf{x}_f = \mathbf{U}^T\mathbf{x}_u$. Note that since $\mathrm{E}[\mathbf{n}_u\mathbf{n}_u^T] = \mathbf{\Lambda}$, the samples of $\mathbf{x}_u$ are decorrelated.

The test statistic is the filtered signal energy:

$$\text{decide } \mathcal{H}_1 \text{ if } \quad L_{bpe}(\mathbf{x}) = \mathbf{x}_f^T\mathbf{x}_f = \mathbf{x}_u^T\mathbf{U}\mathbf{U}^T\mathbf{x}_u = = \mathbf{x}_u^T\mathbf{x}_u = \sum_{i=1}^{N}(\mathbf{x}_u)_i^2 > \gamma. \tag{5.2}$$

The sum terms $(\mathbf{x}_u)_i^2$ are independent by construction and we can apply the central limit theorem with Lyapunov condition [9] to approximate the PDF of test statistic (5.2), supposing that N is large enough. In this case, $L_{bpe}(\mathbf{x})$ will be normally distributed with mean and variance equal to $\sum_{i=1}^{N}\mathrm{E}[(\mathbf{x}_u)_i^2]$ and $\sum_{i=1}^{N}\mathrm{var}[(\mathbf{x}_u)_i^2]$ respectively. Defining the filtered signal energy $E_f = \mathbf{s}_f^T\mathbf{s}_f$, we find

$$\begin{aligned} L_{bpe}(\mathbf{x}) &\sim \mathcal{N}\big(\mathrm{Tr}(\mathbf{C}), 2\mathrm{Tr}(\mathbf{C}^2)\big) \quad \text{under } \mathcal{H}_0 \\ L_{bpe}(\mathbf{x}) &\sim \mathcal{N}\big(E_f + \mathrm{Tr}(\mathbf{C}), 4\mathbf{s}_f^T\mathbf{C}\mathbf{s}_f + \\ &\quad + 2\mathrm{Tr}(\mathbf{C}^2)\big) \quad \text{under } \mathcal{H}_1. \end{aligned} \tag{5.3}$$

The covariance matrix of $\mathbf{n}$ is $\sigma^2\mathbf{I}$ and thus $\mathbf{C} = \sigma^2\mathbf{H}\mathbf{H}^T$. Finally, the ROC curve for this detector can be calculated as follows:

$$\begin{aligned} P_d(\gamma) &= Q\left(\frac{\gamma - E_f - \mathrm{Tr}(\mathbf{C})}{\sqrt{4\mathbf{s}_f^T\mathbf{C}\mathbf{s}_f + 2\mathrm{Tr}(\mathbf{C}^2)}}\right), \\ P_{fa}(\gamma) &= Q\left(\frac{\gamma - \mathrm{Tr}(\mathbf{C})}{\sqrt{2\mathrm{Tr}(\mathbf{C}^2)}}\right). \end{aligned} \tag{5.4}$$

6 Numerical example

We now give an example of the ROC curves discussed in the paper. The parameters' orders of magnitude are determined from a real knock signal. The values taken are the following: P =3, θ_1 = [1.0, -2.3·10^5 Hz/s, 7 kHz, 3.9, 0.61 ms, 0.6 ms]^T, θ_2 = [0.8, -2.8·10^5 Hz/s, 12 kHz, 1.1, 0.64 ms, 0.56 ms]^T, θ_3 = [0.5, -3.2·10^5 Hz/s, 17 kHz, 5.7, 0.67 ms, 0.57 ms]^T, N =167 (corresponding to 10°–50° crank angle window at 3000 RPM and 75 kHz sampling frequency). Figure 2 shows the ROC curves for signal-to-noise ratio of -6 dB. The filter $\mathbf{H}$ from (5.1) is a 50-point finite impulse response approximation of a second order infinite impulse response filter with quality factor 2.3, centered on β_1 (the strongest resonance).

As we see, the model of actual knock detection scheme is quite far below the NP bound, showing that there is space left for possible performance improvement. This can be explained by the fact that bandpass filtering is a non-coherent treatment where

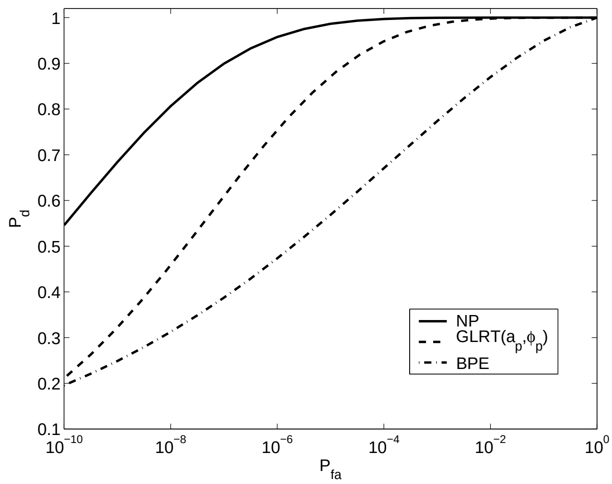

Figure 2: ROC curves for SNR=-6 dB.

the integration gain does not increase with sample size. To illustrate the results, suppose that a detection probability of 0.9 is prescribed. In this case, there is a P_{fa} gain factor of ≈10^3 between BPE and GLRT(a_p, ϕ_p). For a 4-cylinder engine running at 3000 RPM without knock, the number of false alarms passes from 136 to 0.13 per minute. Since false alarms engage a useless spark advance correction and thus engine efficiency decrease, this is considerable.

7 Conclusions

The present document considered the standard engine knock detection processing system. Based on a simple signal model, analytical results for detector performance were derived in terms of receiver operating characteristic. They were compared to the theoretical upper bound given by the Neyman-Pearson test, as well as to the ROC curve of the case with unknown amplitudes and phases. The results show how much performance improvement can be expected. To exploit this option, our further investigations will consider the usage of a priori knowledge on unknown parameters and/or their estimation.

References

[1] J.B. Heywood. *Internal Combustion Engine Fundamentals*. McGraw-Hill, 1988.

[2] B. Samimy and G. Rizzoni. Time-frequency analysis for improved detection of internal combustion engine knock. In *Proceedings of the IEEE-SP International Symposium on Time-Frequency and Time-Scale Analysis*, Philadelphia, October 1994.

[3] S. Carstens-Behrens, M. Urlaub, J.F. Böhme, J. Forster, and F. Raichle. FEM approximation of internal combustion chambers for knock investigations. In *Proceedings of the World Congress & Exhibition*, Detroit, March 2002.

[4] B. Samimy, G. Rizzoni, A. Sayeed, and D.L. Jones. Design of training data-based quadratic detectors with application to mechanical systems. In *Proceedings of the IEEE ICASSP*, Atlanta, May 1996.

[5] LJ. Stanković and J.F. Böhme. Time-frequency analysis of multiple resonances in combustion engine signals. *Signal Processing*, 79(1), November 1999.

[6] N. Härle and J.F. Böhme. Detection of knocking for spark ignition engines based on structural vibrations. In *Proceedings of the IEEE ICASSP*, Dallas, April 1987.

[7] M. Urlaub and J.F. Böhme. Reconstruction of pressure signals on structure-borne sound for knock investigation. In *Proceedings of the SAE World Congress*, Detroit, March 2004.

[8] S.M. Kay. *Fundamentals of Statistical Signal Processing*, volume II : Detection Theory. Prentice-Hall, 1993.

[9] M.G. Kendall. *The Advanced Theory of Statistics*, volume I. Hafner Publishing Company, New York, 1952.